Available online at www.sciencedirect.com
ScienceDirect
Journal of Theoretical Biology 246 (2007) 113–128
Journal of Theoretical Biology
www.elsevier.com/locate/yjtbi

Control of *Streptococcus pyogenes* virulence: Modeling of the CovR/S signal transduction system

Alexander Y. Mitrophanov[a], Gordon Churchward[b], Mark Borodovsky[a,c,*]

[a]*School of Biology, Georgia Institute of Technology, Atlanta, GA 30332-0230, USA*
[b]*Department of Microbiology and Immunology, Emory University School of Medicine, Atlanta, GA 30322, USA*
[c]*Wallace H. Coulter Department of Biomedical Engineering, Georgia Institute of Technology and Emory University, Atlanta, GA 30332-0535, USA*

Received 3 July 2006; received in revised form 6 October 2006; accepted 13 November 2006
Available online 21 November 2006

Abstract

The CovR/S system in *Streptococcus pyogenes* (Group A Streptococcus, or GAS), a two-component signal transduction/transcription regulation system, controls the expression of major virulence factors. The presence of a negative feedback loop distinguishes the CovR/S system from the majority of bacterial two-component systems. We developed a deterministic model of the CovR/S system consisting of eight delay differential equations. Computational experiments showed that the system possessed a unique stable steady state. The dynamical behavior of the system showed a tendency for oscillations becoming more pronounced for longer but still biochemically realistic delays resulting from reductions in the rates of translation elongation. We have devised an efficient procedure for computing the system's steady state. Further, we have shown that the signal–response curves are hyperbolic for the default parameter values. However, in experiments with randomized parameters we demonstrated that sigmoidality of signal–response curves, implying a response threshold, is not only possible, but seems to be rather typical for CovR/S-like systems even when binding of the CovR response regulator protein to a promoter is non-cooperative. We used sensitivity analysis to simplify the model in order to make it analytically tractable. The existence and uniqueness of the steady state and hyperbolicity of signal–response curves for the majority of the variables was proved for the simplified model. Also, we found that provided CovS was active, the system was insensitive to changes in the concentration of any other phosphoryl donor such as acetyl phosphate.

Keywords: Signal transduction network; Two-component system; Signal–response curve; Transcription regulation control

1. Introduction

For a bacterium to adapt and survive it must acquire and process information flows coming from the surrounding environment. These flows consist of series of signals produced by changes in pH, light intensity, osmolarity, concentration of small molecules, etc. Bacteria have evolved molecular systems specialized for transmitting these signals into the cell and triggering a response by causing changes in the expression levels of target genes. A large class of signal transduction systems, called two-component systems (reviewed in Stock et al., 2000; West and Stock, 2001; Kenney, 2002; Harshey et al., 2003), include two major players—a sensor kinase and a response regulator. When the signal is received, the sensor kinase phosphorylates the response regulator, thus modulating the DNA-binding properties of the latter, and determines which genes will be affected by the external signal. Besides prokaryotes, this two-component mechanism of signal transduction has been found in archaea, plants, fungi, and protozoans (Koretke et al., 2000).

Two-component systems play a variety of roles in bacterial cells. *Streptococcus pyogenes* (Group A Streptococcus, or GAS) is an important human pathogen that causes diseases ranging from superficial infections such as pharyngitis and pyoderma to life-threatening invasive

*Corresponding author. School of Biology, Georgia Institute of Technology, Atlanta, GA 30332-0230, USA. Tel.: +1 404 894 8432; fax: +1 404 894 0519.
E-mail address: mark.borodovsky@biology.gatech.edu (M. Borodovsky).

0022-5193/$ - see front matter © 2006 Elsevier Ltd. All rights reserved.
doi:10.1016/j.jtbi.2006.11.009

diseases such as toxic shock syndrome and necrotizing fasciitis (Cunningham, 2000). The CovR/S (also termed CsrR/S) system determines the response of GAS to stresses such as increased temperature, salt concentration, and decreased pH (Dalton and Scott, 2004). It regulates the expression of ~15% of GAS genes (Graham et al., 2002). The CovR/S system controls directly the expression of major virulence factors (Bernish and Rijn, 1999; Miller et al., 2001; Federle and Scott, 2002; Gao et al., 2005; Gusa and Scott, 2005; Sumby et al., 2006) and is an important factor in the transition from colonization to invasion. The CovR/S system, whose major components are the sensor kinase CovS and the response regulator CovR, has several important features. First, it represents regulatory systems ubiquitous in prokaryotes (Parkinson, 1993; Stock et al., 2000), including all major bacterial human pathogens. Second, unlike most other two-component regulatory systems (such as e.g. PhoP/Q and PmrA/B (Groisman, 2001), KdpD/E (Kremling et al., 2004), and NtrB/C (Cullen et al., 1996)), the response regulator (CovR) acts primarily to repress rather than activate gene expression (Graham et al., 2002). Third, the system contains a negative feedback loop (Gusa and Scott, 2005). Fourth, the available genetic evidence suggests that the *cov* regulon can respond to internal metabolic signals as well as external environmental signals (Heath et al., 1999; Graham et al., 2002; Dalton and Scott, 2004). Therefore the CovR/S system is an important target for computational analysis of the quantitative behavior of bacterial transcription control systems, for both practical and theoretical reasons.

Currently, quantitative modeling of transcription control systems is a well-established field (Smolen et al., 2000; Hasty et al., 2001; de Jong, 2002). Early attempts to describe gene regulation focused on the mathematical properties of simplified models, utilizing the formalism of ordinary differential equations (ODEs) (Goodwin, 1965; Griffith, 1968a, b). Later, it was recognized that the non-zero durations of transcription, translation, and diffusion should be taken into account (Banks and Mahaffy, 1978; Tyson and Othmer, 1978; Bliss et al., 1982), leading to the development of models using delay differential equations (DDEs) and the study of properties of these models such as the stability of the steady state, the possibility of oscillations, and the existence of multiple steady states (Banks and Mahaffy, 1978; Tyson and Othmer, 1978; Bliss et al., 1982; Smith, 1987).

The ODE/DDE approach has been applied to model the behavior of real systems such as the growth of the phage T7 in *E. coli* (Endy et al., 1997), the expression of the tryptophan operon in *E. coli* (Santillan and Mackey, 2001), and the *E. coli* lactose operon (Yildirim and Mackey, 2003; Mackey et al., 2004; Yildirim et al., 2004) with excellent agreement between the models' predictions and experimental observations.

Results on quantitative modeling of signal transduction have been reviewed by Ashtagiri and Lauffenburger (2000). As with gene regulation modeling, one segment of the existing literature concentrates on theoretical properties of signal transduction models, such as the possibility of oscillatory behavior (Kholodenko, 2000; Saez-Rodriguez et al., 2004), bistability (Ferrell and Xiong, 2001), modularity (Saez-Rodriguez et al., 2004), and signal amplification (Kholodenko et al., 1997; Heinrich et al., 2002), while the other segment is devoted to bridging the gap between theory and experiment. A considerable body of the literature is focused on signal transduction systems in eukaryotic cells, such as the cascades of MAPK kinases (Huang and Ferrell, 1996; Bhalla and Iyengar, 1999; Kholodenko, 2000; Asthagiri and Lauffenburger, 2001; Schoeberl et al., 2002; Saez-Rodriguez et al., 2004). The corresponding models are ODE systems describing mass action (or Michaelis–Menten) kinetics, and model predictions compare favorably with experiment (Schoeberl et al., 2002). In prokaryotes, researchers' attention has mostly focused on two-component signal transduction systems *per se*, without taking into account the associated transcription regulation modules (Alves and Savageau, 2003; Batchelor and Goulian, 2003; Rao et al., 2004, 2005). Two papers which explicitly accounted for both signal transduction and transcription regulation described an ODE model of the KdpD/E system in *E. coli* (Kremling et al., 2004; Saez-Rodriguez et al., 2005). The model showed a good fit to the experimental data in vivo and in vitro (Kremling et al., 2004). However, the KdpD/E system involves a positive feedback loop rather than a negative feedback loop, such as the one possessed by the CovR/S system. Further, for transcription regulation systems, DDEs have been shown to be more suitable models than ODEs (Banks and Mahaffy, 1978; Bliss et al., 1982; Yildirim and Mackey, 2003). Finally, the standard way to represent the interactions of regulatory proteins with DNA in gene expression control system has been through the use of Hill-like curves, following the early developments of Yagil and Yagil (1971). However, Hill curves have been criticized for their empirical nature (Hill, 1985). It is therefore necessary to devise more advanced models for describing the interactions between regulators and DNA in transcription control systems.

In this paper, we develop a DDE model for the CovR/S system in GAS, drawing upon the available knowledge about the system and the existing methodology for modeling transcription regulation systems. While the model focuses on the key components of the CovR/S system, it can be readily extended to include other components, and even modified to describe systems with positive feedback loops. In the model, we assume that CovR-binding sites are independent, but a more general binding mechanism can be easily incorporated into the model framework. (See Supplementary material for a quantitative description of repression of transcription in the case of general binding mechanism, with or without cooperativity—Appendix B.) Our primary goal was to investigate the transient and steady-state behavior, concentrating on the properties related to the signal transduc-

tion function. We utilize an existing algorithm to model the transient dynamics, and devise an effective procedure to determine steady-state concentrations of the model components. This procedure is instrumental for our computational investigation of hyperbolicity and sigmoidality of the steady-state signal–response curves. Using sensitivity analysis techniques, we were able to derive a simplified model which permits analytical investigation. For this reduced model, we rigorously prove the existence and uniqueness of the steady state, and some general characteristics of the signal–response curves. The approach that we develop elucidates the universal properties of two-component systems with a negative feedback loop, and is suitable for analysis of other types of prokaryotic signal transduction systems.

2. Model description

We delineate the deterministic model of the CovR/S system, which describes the behavior of the system averaged over a population of cells (so that the stochastic effects resulting from small numbers of participating molecules can be neglected). We have also developed a general model describing gene repression with arbitrary degree of cooperativity in binding of the repressor to DNA. For the parameters of the model, we chose a set of biologically justifiable values (Tables 1 and 2), utilizing experimental data obtained for the CovR/S system, and data from the literature.

A schematic of the CovR/S system, featuring the key components reflected in our model, is shown in Fig. 1. The key signal transduction reactions in which CovR and CovS participate are as follows:

(I) $\mathrm{CovS} + \mathrm{ATP} \overset{k_1/k_{-1}}{\longleftrightarrow} \mathrm{CovS\text{-}P} + \mathrm{ADP}$ (autophosphorylation),

(II) $\mathrm{CovR} + \mathrm{CovS\text{-}P} \overset{k_2/k_{-2}}{\longleftrightarrow} \mathrm{CovS} + \mathrm{CovR\text{-}P}$ (phosphotransfer).

Here, CovR-P and CovS-P are the phosphorylated forms of CovR and CovS, P is the phosphoryl group, and k_i, $i = 1, -1, 2, -2$, are the reaction rates. The autophosphorylation in Reaction 1 is signal dependent: the rate of the forward reaction is linked to the intensity of the incoming signal. As it has been shown that CovS-P is not necessary for the phosphorylation of CovR in vivo (Dalton and Scott, 2004), we assume the existence of a phosphate donor X-P, which transfers the phosphoryl group to CovR in the reaction

(III) $\mathrm{CovR} + \mathrm{X\text{-}P} \overset{k_3}{\longrightarrow} \mathrm{CovR\text{-}P} + \mathrm{X}.$

We also assume that CovR-P and CovS-P can be dephosphorylated via hydrolysis as follows:

(IV) $\mathrm{CovR\text{-}P} \overset{k_4}{\longrightarrow} \mathrm{CovR} + \mathrm{P}.$

(V) $\mathrm{CovS\text{-}P} \overset{k_5}{\longrightarrow} \mathrm{CovS} + \mathrm{P}.$

Reactions 4 and 5 are pseudo-first-order reactions. The remaining reactions represented in the model are as follows: (VI) synthesis of CovR and CovS mRNA; (VII) decay of CovR and CovS mRNA; (VIII) synthesis of CovR; (IX) decay of CovR; (X) synthesis of CovS; (XI) decay of CovS. Since the CovS and CovR come from the same initial transcript (Gusa and Scott, 2005), the corresponding rate and equilibrium constants are the same. However, we distinguish between the CovR and CovS mRNA, because the expressions for the rate of their

Table 1
Parameter values for the model equations

k_1	$0.6\ (\mu M)^{-1}$	k_{10}	$500\ h^{-1}$
k_{-1}	$2e{-}7\ (\mu M)^{-1}$	k_{11}	$300\ h^{-1}$
k_2	$600\ (\mu M)^{-1}$	k_{12}	$50\ \mu M\ h^{-1}$
k_{-2}	$24e{-}9\ (\mu M)^{-1}$	k_{13}	$20\ h^{-1}$
k_3	$0.04\ (\mu M)^{-1}$	k_{14}	$550\ h^{-1}$
k_4	$1500\ h^{-1}$	k_{15}	$250\ h^{-1}$
k_5	$300\ h^{-1}$	K_6	$0.4\ (\mu M)^{-1}$
k_6	$60\ \mu M\ h^{-1}$	K_{12}	$0.8\ (\mu M)^{-1}$
k_7	$8\ h^{-1}$	ATP	$2000\ \mu M$
k_8	$400\ h^{-1}$	ADP	$250\ \mu M$
k_9	$200\ h^{-1}$	XP	$50\ \mu M$
M_6	5	m_{12}	5

Table 2
Transcriptional and translational delays

covR transcription time (transcriptional delay for CovS mRNA)	0.005 (h)
CovR translation time	0.004
CovS translation time	0.009
Has translation time	0.008

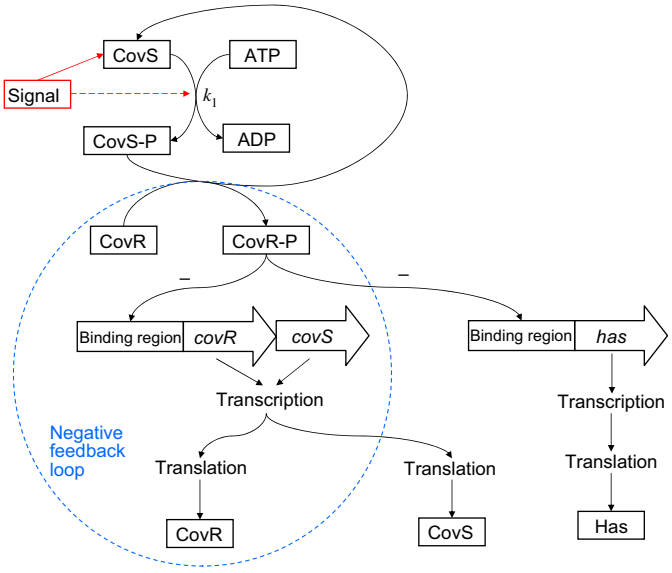

Fig. 1. A schematic of the CovR/S signal transduction system. The blue circle indicates the negative feedback loop associated with CovR.

Table 3
Reactants and the corresponding concentration variables

CovS	CovS-P	CovR	CovR-P	CovR mRNA	CovS mRNA	Has mRNA	Has
X_1	X_2	X_3	X_4	X_5	X_6	X_7	X_8

synthesis include different delays (zero delay for CovR mRNA, and non-zero delay for CovS mRNA). The decay reactions are first-order reactions. The protein synthesis reactions are pseudo-first-order reactions with rates proportional to the concentration of the corresponding mRNA. In this study we include in the system just one target gene and the corresponding protein. We chose Has, representing the proteins involved in GAS hyaluronic acid capsule synthesis. (The *has* operon contains three genes, *hasA*, *hasB*, and *hasC*. Our "Has" notation stands for HasA.) We thus need to include four more reactions: (XII) synthesis of Has mRNA; (XIII) decay of Has mRNA; (XIV) synthesis of Has; (XV) decay of Has. The rate constants for Reactions (VI–XV) are denoted by k_i, where i is the reaction number as given above.

The available evidence suggests that CovR must be phosphorylated to regulate gene expression in vivo (Dalton and Scott, 2004). For the rates of the mRNA synthesis reactions we used expressions of the following form:

$$Rate = k_i/(1 + K_i[\text{CovR-P}])^5,$$

where k_i, $i = 6,12$, is the synthesis rate in the absence of repression, and K_i is the equilibrium binding constant for CovR-P and a binding site of the corresponding gene (see Supplementary material for derivations, Appendix B). The exponent in the denominator reflects the multiplicity of the independent transcription factor binding sites for a given gene. The *has* promoter is known to contain five independent sites for binding CovR-P (Federle and Scott, 2002); we assumed the same regulation scheme for *covRS*.

With the reactant concentrations denoted by $X_1,\ldots,X_8$ (see Table 3), the reactions described above give rise to the system of DDEs:

$$\begin{aligned} dX_1/dt = {} & k_{-1}[\text{ADP}]X_2 + k_2X_2X_3 + k_5X_2 + k_{10}X_6^{(d_6)} \\ & - k_1[\text{ATP}]X_1 - k_{-2}X_1X_4 - k_{11}X_1, \end{aligned} \quad (1)$$

$$\begin{aligned} dX_2/dt = {} & k_1[\text{ATP}]X_1 + k_{-2}X_1X_4 - k_{-1}[\text{ADP}]X_2 \\ & - k_2X_2X_3 - k_5X_2, \end{aligned} \quad (2)$$

$$\begin{aligned} dX_3/dt = {} & k_{-2}X_1X_4 + k_4X_4 + k_8X_5^{(d_5)} - k_2X_2X_3 \\ & - k_3[\text{X-P}]X_3 - k_9X_3, \end{aligned} \quad (3)$$

$$dX_4/dt = k_2X_2X_3 - k_{-2}X_1X_4 + k_3[\text{X-P}]X_3 - k_4X_4, \quad (4)$$

$$dX_5/dt = k_6/(1 + K_6X_4)^5 - k_7X_5, \quad (5)$$

$$dX_6/dt = k_6/(1 + K_6X_4^{(d_4)})^5 - k_7X_6, \quad (6)$$

$$dX_7/dt = k_{12}/(1 + K_{12}X_4)^5 - k_{13}X_7, \quad (7)$$

$$dX_8/dt = k_{14}X_7^{(d_7)} - k_{15}X_8. \quad (8)$$

In this model, the concentrations [ATP], [ADP], and [X-P] are assumed to be constant. While all the reactions are catalyzed by enzymes, and certain intermediate complexes are formed, in order to keep the system tractable, we omit the intermediate stages and reactants that should not make a significant impact on the system.

In Eqs. (1)–(8), the superscript d_i, $i = 4, \ldots, 7$, denotes that the corresponding system variable has a delayed argument. For example, the rate of CovR synthesis in Eq. (3) has the form $k_8X_5(t-\tau)$, where τ is the average time of the CovR mRNA translation. All the terms describing mRNA translation have delays which reflect the translation times for the corresponding proteins. As for transcription, only the term for CovS mRNA synthesis (Eq. (6)) has a delayed argument, since the *covS* gene is located downstream of *covR*, and transcription of the former cannot start until the latter is transcribed. Here, the delay equals the transcription time for the CovR mRNA. The rates of CovR mRNA and Has mRNA synthesis enter Eqs. (5) and (7) with zero delays, since the corresponding genes are the most upstream genes in their operons, and the mRNA translation starts almost immediately after transcription initiation.

3. Methods

All computations and visualization were performed in MATLAB R2006a.

3.1. The steady-state equations and their solution

The steady-state equations have the form (we rearranged some terms in the equations):

$$\begin{aligned} k_{-1}[\text{ADP}]X_2 + k_2X_2X_3 + k_5X_2 + k_{10}X_5 = {} & k_1[\text{ATP}]X_1 \\ & + k_{-2}X_1X_4 + k_{11}X_1, \end{aligned} \quad (9)$$

$$k_{-1}[\text{ADP}]X_2 + k_2X_2X_3 + k_5X_2 = k_1[\text{ATP}]X_1 + k_{-2}X_1X_4, \quad (10)$$

$$k_2X_2X_3 + k_3[\text{X-P}]X_3 + k_9X_3 = k_{-2}X_1X_4 + k_4X_4 + k_8X_5, \quad (11)$$

$$k_2X_2X_3 + k_3[\text{X-P}]X_3 = k_{-2}X_1X_4 + k_4X_4, \quad (12)$$

$$k_6/(1 + K_6X_4)^5 = k_7X_5, \quad (13)$$

$$k_{12}/(1+K_{12}X_4)^5 = k_{13}X_7, \tag{14}$$

$$k_{14}X_7 = k_{15}X_8. \tag{15}$$

We did not include the steady-state version of Eq. (6) since it is similar to Eq. (13), and used the steady-state equality $X_5 = X_6$. Thus, we exclude X_6 from our steady-state analyses. Subtracting Eq. (10) from Eq. (9), we get

$$k_{10}X_5 = k_{11}X_1. \tag{16}$$

Subtracting Eq. (12) from Eq. (11), we obtain

$$k_8X_5 = k_9X_3. \tag{17}$$

Eq. (13) yields the expression for X_4 in terms of X_5:

$$X_4 = \left(\sqrt[5]{\frac{k_6}{k_7X_5}} - 1\right)/K_6. \tag{18}$$

Note that, for Eq. (18) to be valid, we should have

$$X_5 < \frac{k_6}{k_7}. \tag{19}$$

Using Eqs. (14) and (15) in combination with Eq. (19), we can obtain expressions for X_7 and X_8 in terms of X_5. From Eq. (10), we get

$$X_2 = \frac{k_1[\mathrm{ATP}]X_1 + k_{-2}X_1X_4}{k_{-1}[\mathrm{ADP}] + k_2X_3 + k_5}. \tag{20}$$

Combining Eqs. (16)–(18) and (20), we can express X_2 in terms of X_5. If we plug the expressions for X_1, …, X_4 in terms of X_5 into Eq. (12), we obtain an algebraic equation for X_5, which is to be solved on interval $(0, k_6/k_7)$. The number of solutions of this equation determines the number of solutions of system (9)–(15), because all the other variables are uniquely expressed in terms of X_5. We are only interested in non-negative solutions of system (9)–(15), since only non-negative values for the concentrations are biologically relevant. It is easy to see that, if X_5 is positive, then all other concentrations are positive.

Due to the complex structure of the model, theoretical investigation of the question of existence and uniqueness of solutions of the above-mentioned equation for X_5 seems unfeasible. When finding the solution, we assumed its existence and uniqueness, in accordance with our hypothesis discussed in the Results section. We located the steady state by solving the equation for X_5 (which has the form $f(X_5) = 0$)) using MATLAB's function fzero, given that $f(0)$ and $f(k_6/k_7)$ have different signs, which can be tested directly.

The method outlined above is suitable for systems with different binding site multiplicities. In the computational analysis of the steady-state signal–response curves, we also considered the versions of the CovR/S model with cooperative binding of CovR-P (see the Results section). The strategy we used to solve the corresponding steady-state equations is similar to the one described above. The only difference is that the Eqs. (13)–(14) are replaced with their sigmoidal counterparts.

3.2. Computational analysis of signal–response curves

To analyze hyperbolicity and sigmoidality of signal–response curves we calculated the dependencies of the steady-state concentrations on k_1 for sets of randomly selected K_6, K_{12}, m_6, m_{12}, where m_6 and m_{12} are the Hill coefficients for *covRS* and *has* in the cooperative case (described in the Results section) and the binding site multiplicities in the non-cooperative (default) case. The values of K_6 and K_{12} were taken from interval (0, 5); m_6 and m_{12} were taken from interval (1, 10). The variable k_1 was changing from 0.005 to 10 with step 0.005. A total of 5000 dependencies (signal–response curves) were generated for each of the X_i variables in the cooperative case, and another 5000 in the non-cooperative case. When generating the dependencies, we filtered out the results for which at least one of the functions $X_i(k_1)$ had two consecutive identical values of the absolute value of the derivative. This alleviated computational difficulties which could have arisen when searching for the maxima of the derivative's absolute value. The approximate value of the derivative $X_i'(k_1)$ was calculated as $(X_i(k_1+step)-X_i(k_1))/step$. The maxima were defined as the points k_1 such that the conditions $|X_i'(k_1 - step)| < |X_i'(k_1)|$ and $|X_i'(k_1+step)| < |X_i'(k_1)|$ hold simultaneously. To determine the multiplicities for the local maxima of the derivative's absolute value, we used the following rule: the local maxima within the distance of $2\times step$ from each other were treated as one maximum. The purpose of this restriction was to account for spurious local maxima resulting from computational errors.

We generated two additional sets of 5000 randomly selected K_6, K_{12}, m_6, m_{12} (changing in the same ranges), and used the procedure described above to analyze the maxima of the derivative's absolute value for the function $X_8(X_4)$ in the cooperative and non-cooperative cases. The function was defined by plotting $X_8(k_1)$ against $X_4(k_1)$, where k_1 was changing as above. To plot Figs. 8–10, we used the same definitions of derivative and step 0.0001, but intervals for k_1 were different ($k_1 \in (0.001, 8.1)$ for Fig. 8; $k_1 \in (0.001, 2.1)$ for Fig. 9; $k_1 \in (0.001, 10.1)$ for Fig. 10).

3.3. Sensitivity computations

The sensitivities of the system with respect to changes in the parameters are defined as

$$s_{ij} = \partial C_i/\partial p_j,$$

where C_i, $i = 1, \ldots, n$, are the model's variables (concentrations of the reactants), and p_j, $j = 1,\ldots, m$, are the model's parameters (in our case, the rate constants and equilibrium constants). Such sensitivities are typically studied for the steady-state concentrations, but a generalization of this analysis to the transient phase is also possible (Heinrich and Schuster, 1996; Ingalls and Sauro, 2003). The logarithmic, or relative, sensitivities are defined as follows:

$$\hat{s}_{ij} = \partial \log C_i/\partial \log p_j = (p_j/C_i)s_{ij}.$$

While some researchers consider relative sensitivities a more natural measure of sensitivity, the choice remains to a large extent a matter of individual preference (Heinrich and Schuster, 1996; Varma et al., 1999). Thus, we decided to consider both absolute and relative sensitivities, and use sensitivity coefficients to select candidate reactions for exclusion.

For all the rate and equilibrium constants in system (1)–(8), we computed the steady-state aggregate sensitivity (s_j) and relative sensitivity ($\hat{s}_j$) indicators (see Supplementary Table 1, Appendix B). The aggregate steady-state sensitivity indicators are defined by

$$s_j = \max_i |s_{ij}|, \quad \hat{s}_j = \max_i |\hat{s}_{ij}|.$$

To compute the sensitivities, we used an approximation of the derivative similar to the one used in the signal–response curve analysis, with step 10^{-10}. While the s_j were the highest for k_1 and K_6 (notably larger than the rest of the s_j), the s_j for most other parameters were quite small (less than 0.01), which made it difficult to select the reactions to be excluded. We then turned to the analysis of the relative sensitivities, which allowed us to characterize k_{-1}, k_{-2}, and k_3 as the parameters with lowest sensitivity. For these parameters, the quantities $\hat{s}_j$ were smaller than 0.005; all the other parameters had $\hat{s}_j$ greater than 0.1. Since the value 0.01 for a relative sensitivity can be considered as the threshold below which the corresponding reaction can be excluded (Varma et al., 1999), we selected k_{-1}, k_{-2}, and k_3 as primary candidates to be set to 0. The next step was to test if elimination of the corresponding reactions from the model would change considerably the model's dynamics. To this end, we carried out computational experiments comparing the solutions of the full model and the reduced model (with $k_{-1} = k_{-2} = k_3 = 0$) on the time interval [0, 3] (time in hours). The approximation error, ε, for the reduced and full models in the transient state was calculated as follows:

$$\varepsilon = \max_t \max_i (|X_i(t) - \tilde{X}_i(t)|/X_i(t)) \times 100\%,$$

where $X_i(t)$ and $\tilde{X}_i(t)$, $i = 1, \ldots, 8$, $t \in [0, 3]$, are the reactant concentrations for the full and reduced models, respectively. For the steady-state concentrations, we used a similar expression (without maximization over time). For the default values of the parameters, the approximation error was ~1.2%, which is quite small; for the steady-state values, the error was 0.2%. For delays increased sevenfold, the approximation error did not change. Since $\hat{s}_j$ for k_3 was orders of magnitude larger than that for k_{-1} and k_{-2}, we also estimated the system reduction accuracy for smaller values of k_3. If $k_3 = 0.0004$ (100 times smaller than the default value), the approximation error was found to be 0.012%. If our original model had $k_3 = 0$ (a reasonable approximation for other signal transduction systems, see e.g. (Kremling et al., 2004)), then the only modification required for the reduced system would be $k_{-1} = k_{-2} = 0$. In this situation, the error would be on the order of 1×10^{-5}%. Based on these observations, we concluded that the simplified model is a good approximation to the full model, which becomes especially accurate for small k_3.

3.4. Convergence analysis

To evaluate the time of convergence of the system to steady state, we utilized the following strategy. The system was solved on consecutive intervals of length *step*, until the max-norm of the difference between the solutions at the end-points of two consecutive steps was not larger than the threshold *accuracy*. Next, we selected the time interval of length 2 starting at the last analyzed time point, T, and selected 1000 equally spaced time points in this interval. If the max-norm of the difference of the solution at T and the solutions at each of those 1000 points was not greater than *accuracy*, we reported T as the convergence time. Else, we continued integration by steps of size *step*, until the above conditions were met. In our estimates of convergence times for the system discussed in the test, we used the parameter values $step = 0.05$, $accuracy = 0.01$. To estimate the convergence time averaged over different initial states, we performed 3000 experiments with initial values for the system's variables sampled independently from the uniform distribution on interval (0, 10).

To establish the fact of existence and uniqueness of the steady state, we performed 5000 experiments with randomly selected initial conditions. The initial concentrations were chosen from interval (0, 30). We let the system converge from the default initial state, and then compared the values of the system variables after convergence with the analogous values for the trajectories started at random initial points. To establish convergence, we used the parameter values $step = 0.1$ and $accuracy = 0.003$. The steady states were compared via the max-norm. For the 5000 experiments, the mean max-norm was 0.0015, and the maximum max-norm of the steady-state vector differences was 0.0028. Analogous computations were also performed for the two-variable system (21)–(22). In these experiments, the maximum max-norm was found to be 0.00034, and the average max-norm was 0.00018.

4. Results

4.1. Transient behavior of the model

Since the complexity of system (1)–(8) makes analytic investigation of its properties too difficult, we studied the behavior of system (1)–(8) via computational experiments. Computations were performed in MATLAB using dde23, the function for solving DDEs. The values for the model's parameters were chosen (Tables 1 and 2) based on expert knowledge and upon literature data on signal transduction and transcription regulation systems in *E. coli* (Blat et al., 1998; Yildirim and Mackey, 2003; Kremling et al., 2004). Several parameters were adjusted so as to make the system behavior agree with known experimental facts and

expert opinions; for example, the equilibrium constant for CovR-P binding to the *has* promoter was chosen to make the steady-state concentration of Has on the order of 0.1 μM.

One instance of the system dynamics is shown in Fig. 2. The figure shows convergence to steady state from rather arbitrary initial conditions (Supplementary Table 2, Appendix B). We determined the convergence time to be 0.35 h, which is approximately half the inter-division time for *S. pyogenes* (about 0.75 h in broth at 37 °C). The convergence time averaged over different initial conditions was 0.8 h (coefficient of variation 0.16). We can see that the dynamics of X_5 and X_6 (CovR and CovS mRNA concentrations) are slightly different (near time 0.1 h). However, the negligible differences in the dynamics suggest the possibility of model simplification by exclusion of one of the two variables.

We performed several thousand of computational experiments in which initial concentrations were chosen randomly. In all those experiments, the solutions of Eqs. (1)–(8) showed convergence to the steady state for the initial conditions as in Supplementary Table 2, Appendix B. The stationary concentrations at the steady state were close to the ones found by the algebraic method outlined in Methods. It should be noted that a steady state of system (1)–(8) is also a steady state of the ODE system obtained from Eqs. (1)–(8) by setting the delays equal to 0. This immediately follows from the fact that both the DDE and ODE systems have the same system of steady state equations. By linearizing the ODE system in the vicinity of this steady state and computing the eigenvalues of the coefficient matrix, we have shown that this steady state was stable for the ODE system. Based on these results, we hypothesize that the DDE system (at least for biologically reasonable parameter values) has a stable steady state. Also, since in our experiments all the model's trajectories converged to the same steady state, we conjecture that the steady state of the DDE system is unique.

The presence of delays is one of the distinct features of our model, which makes it different from the signal transduction models considered by other authors. With delays, the behavior of the model becomes more complicated, and the analysis of DDE systems is in general more difficult than that of ODE systems. Although the necessity of incorporating delays is dictated by the biological nature of the processes being modeled, it is desirable to see how important the delays are from the modeling perspective. For that purpose, we compared the dynamics of the DDE model (1)–(8) with that of the corresponding ODE model. The results of this comparison are illustrated by Fig. 3. We see that differences between the trajectories of the systems are substantial for short-time dynamics, and become negligible as t grows to $t \gg \tau$, where τ is the maximum delay parameter in the model. This limiting behavior of the differences was to be expected, since the steady-state solutions of the DDE and the corresponding ODE systems satisfy the same set of equations. The observed results imply that the importance of incorporating time delays into the model depends on the purpose of modeling: if the investigation focuses on long-term behavior, the delays can be neglected. However, in many situations the strength of the signal transmitted by CovR/S may change abruptly, and the induced changes in the cell's behavior are determined by the short-term dynamics of the system. In such cases, time delays should be taken into account.

We studied the reaction of the system to abrupt signal changes by introducing "parameter jumps" for k_1. Fig. 4 shows the dynamics of the system when the system at time $t = 0.2$ h was perturbed by a five-fold increase in the value of k_1 (corresponding to an increase in signal intensity), and then at time $t = 0.9$ h experienced a five-fold decrease in k_1. The initial concentrations were the steady-state concentrations (the limiting ones in Fig. 2). Notably, the times of convergence to the steady states after the first and second

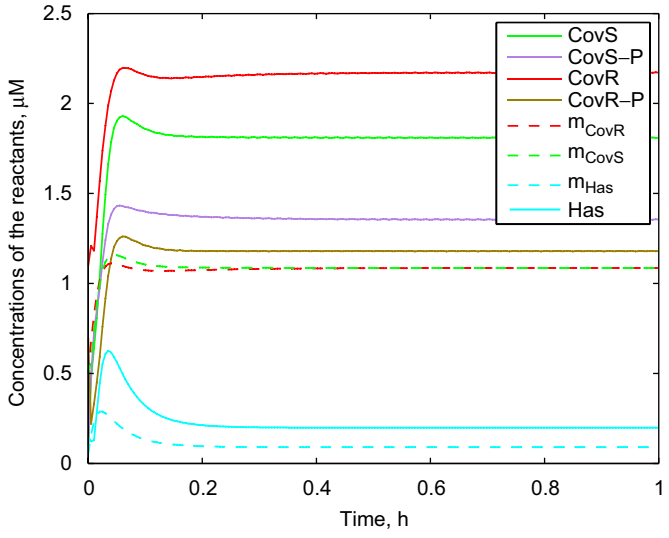

Fig. 2. Dynamics of the DDE model for the CovR/S system.

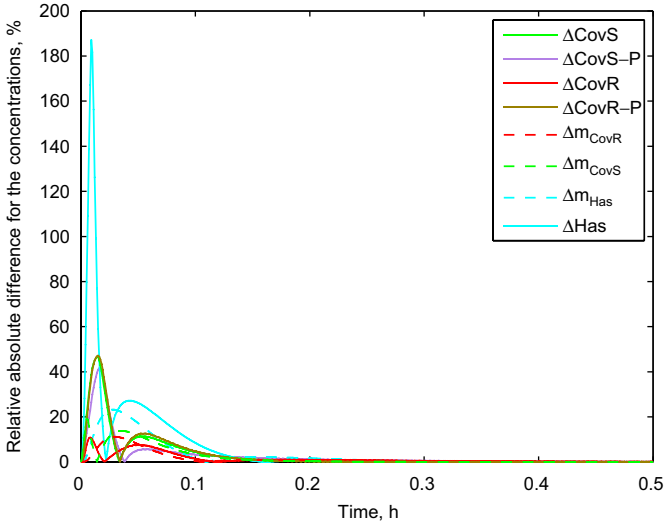

Fig. 3. Comparison of the dynamics of the DDE model for the CovR/S system with the corresponding ODE model (all delays are set to 0).

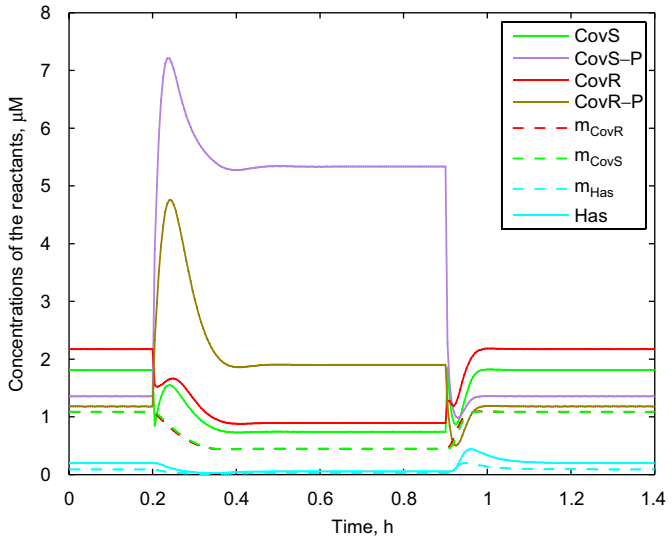

Fig. 4. Dynamics of the DDE model with jump-like changes in the value of k_1 (see text for details).

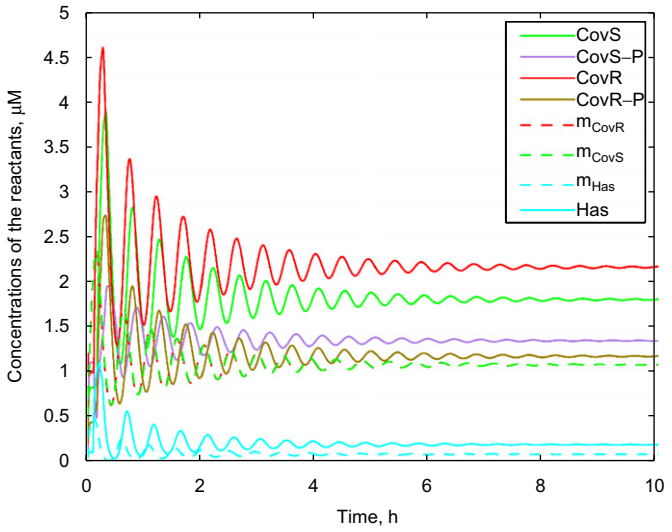

Fig. 6. Dynamics of the CovR/S model for large delays. The translation time for CovR was 0.1 h, the translation time for CovS was 0.15 h, and the translation time for Has was 0.09 h.

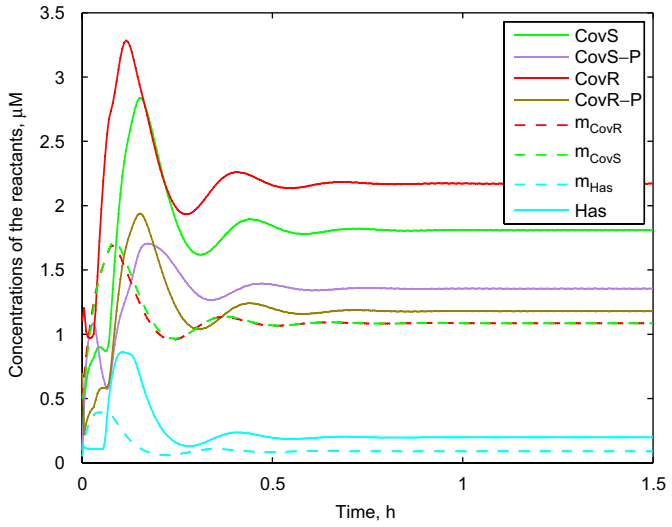

Fig. 5. Dynamics of the system with translational delays increased 7-fold.

jumps (0.35 and 0.3 h, respectively) were quite close to the convergence time for the dynamics shown in Fig. 2.

The discovery of the possibility of oscillations in the systems with delays and negative feedback was an important result in quantitative analysis of dynamical models of transcription regulation systems (Bliss et al., 1982; Smith, 1987; Jensen et al., 2003). Oscillations were also shown to arise in complex eukaryotic signaling circuits such as MAPK cascades (Kholodenko, 2000; Saez-Rodriguez et al., 2004) and other eukaryotic signaling pathways (Bhalla and Iyengar, 1999), as well as in generic models of signal transduction (Soyer et al., 2006). However, the possibility of oscillations in prokaryotic signal transduction systems coupled with transcription regulation remains unexplored. Thus, one of our goals was to determine the conditions under which oscillations (damped or sustained) are possible in the CovR/S system. We were able to show in computational experiments that increases in the magnitude of translational delays does induce damped oscillations in the system. Fig. 5 shows the evolution of the system with translational delays for CovR, CovS and Has increased seven-fold. The convergence time for this system (estimated to be 0.8 h) is notably larger than that for the default delays. Further increase in delays led to more pronounced oscillatory behavior (Fig. 6) and an increase in the damping time (which was estimated to be 10.15 h). The necessity to consider increased delays comes from the observation that, in bacterial cells, "delays on the order of a few minutes are expected between transcription initiation and the formation of the active repressor able to negatively regulate the activity of its own promoter" (Rosenfeld et al., 2002). These results show that oscillations indeed may be possible in the systems similar to Eqs. (1)–(8), as the time of transcription and translation varies among different genes. In eukaryotic cells, the orders of magnitude for the delays can be tens of minutes (Jensen et al., 2003). Thus undamped oscillations can potentially arise in two-component signal transduction/transcription regulation systems in eukaryotes.

4.2. Steady-state analysis

Finding the steady-state concentrations by analyzing the convergence of the solution of Eqs. (1)–(8) in many cases is inconvenient. An easier and faster way would be to solve the steady-state equations implied by Eqs. (1)–(8). The steady state equations can be obtained from Eqs. (1)–(8) by setting the time derivatives equal to zero. We developed an efficient method to solve this system of nonlinear algebraic equations (see Methods).

The steady-state analysis of Eqs. (1)–(8) is especially important when considering the response of the system to the changes in the stimulus intensity (described by the changes in k_1). It is worthwhile to investigate the dependency of the steady-state response level on the intensity of the detected signal. In this setting, we are interested in the response function that defines the steady-state concentration of X_3 (the response regulator CovR) as a function of k_1. Particularly, an important question to ask is whether this signal–response curve is sigmoidal. The notion of curve sigmoidality in the context of biochemical regulation is usually related to the possibility of approximating the curve by the Hill curve with the Hill coefficient greater than 1 (see Supplementary material Appendix B) (Goldbeter and Koshland, 1981; Koshland et al., 1982; Ferrell, 1996; Huang and Ferrell, 1996; Ferrell and Machleder, 1998). Examples of a non-sigmoidal (hyperbolic) and a sigmoidal curves in the case of repressing signal are shown in Fig. 7. Here the equation for the hyperbolic curve is

$$[\text{Response}] = a/(1 + b[\text{Signal}])^5$$

and the equation for the sigmoidal curve is

$$[\text{Response}] = a/(1 + b[\text{Signal}]^5);$$

the values of $a>0$ and $b>0$ were the same in both cases. The equation for the sigmoidal curve is a Hill-type equation with the Hill coefficient 5; see e.g. (Acerenza and Mizraji, 1997). It is easy to see that the sigmoidal function gives a higher response level for weak signal and a lower response level for strong signal than the hyperbolic curve with the same parameters. Hence, the changes in the response values for sigmoidal curves are generally more abrupt than for hyperbolic curves. Although in Fig. 7 we show only the graphs of decreasing functions, both hyperbolic and sigmoidal functions can be increasing; in the context of transcription regulation, increasing signal–response functions correspond to positive regulation. The more general definition of sigmoidality given below is applicable for both decreasing and increasing functions.

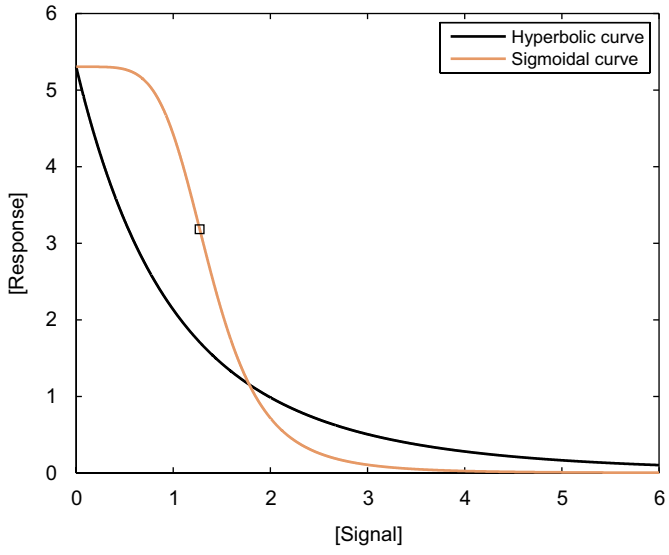

Fig. 7. Hyperbolic and sigmoidal curves (see text for details). The black square on the sigmoidal curve designates the maximum point of the derivative's absolute value.

While the Hill equation-based definition may be sufficient for some practical cases, we find it necessary to consider a more general definition of sigmoidality. We call a function sigmoidal if there are points at which the response function changes between being strictly convex and strictly concave. At some of such points, the steepness (absolute derivative) of the signal–response curve has a local maximum; such points can be regarded as "thresholds". The presence of a threshold implies switch-like properties of the signal transduction system, with subthreshold values of signal intensity defining one level of response, and superthreshold values determining another level. The thresholds of a sigmoidal signal–response curve are means of converting gradual changes in the signal into discrete response; systems with hyperbolic response curves convert gradual input into gradual output. Thus the response structure in the sigmoidal and hyperbolic cases is qualitatively different.

Since the repression of transcription in our model is performed by CovR-P (X_4), the phosphorylated form of CovR, it is of interest to consider the dependency $X_4 = X_4(k_1)$. In addition to the dependencies of X_3 (CovR concentration) and X_4 on k_1, we can also investigate the function $X_8 = X_8(k_1)$, which shows the influence of the signal intensity on the expression of Has (a protein controlled by CovR).

We generated steady-state signal–response curves for all the variables in the system by numerically solving the steady state equations for different values of k_1. These dependencies (Fig. 8) demonstrate hyperbolicity of all the response functions; we established hyperbolicity by verifying that the numerical derivatives of the functions are all monotonic. The signal–response function for CovR (X_3) is a monotonically decreasing function, with $X_3 \to 0$ as $k_1 \to \infty$; for Has (X_8), the picture is similar. Interestingly, the concentration of CovR-P (X_4) grows with k_1, showing that the increase in CovR phosphorylation rate has a greater influence on the CovR-P concentration than the decrease in the speed of CovR synthesis. In the next subsection, we describe the results of our analytic investigation of the signal–response function for a simplified CovR/S model.

In addition to the model (Section 2) with no cooperativity in binding of the regulator protein (CovR-P), we considered a model with cooperative binding of CovR-P to the *covRS* and *has* promoters. In this case, we used Hill-type functions (see Supplementary material Appendix B) for the rate of mRNA synthesis. For example, the expression for the CovR mRNA synthesis rate had the form

$$Rate = \frac{k_6}{1 + K_6[\text{CovR-P}]^{m_6}},$$

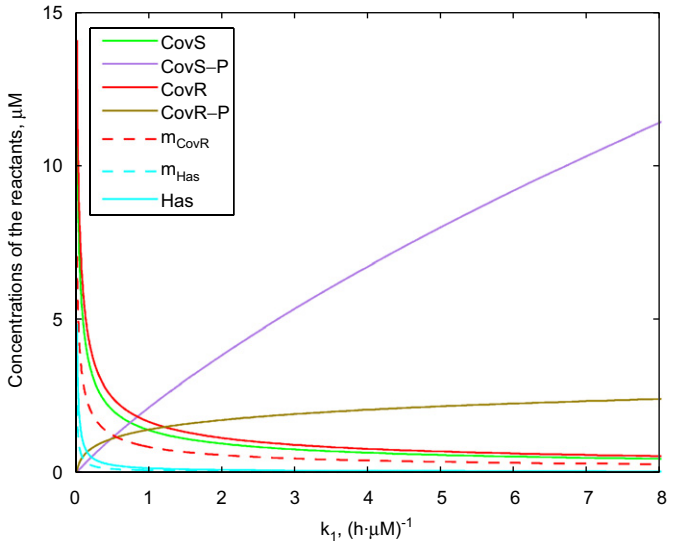

Fig. 8. Dependency of the steady-state values of the model's variables on k_1 (signal–response curves). The dependency for CovS mRNA is not shown since it is identical to that for CovR mRNA.

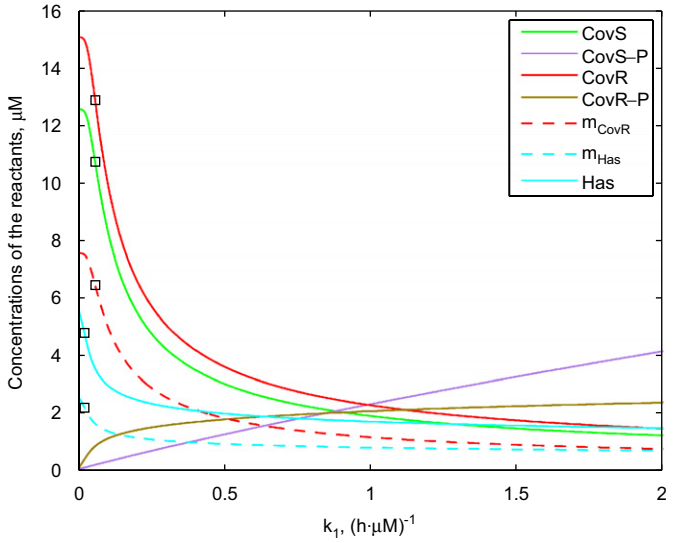

Fig. 9. Dependency of the steady-state values of the model's variables on k_1 (signal–response curves) for the cooperative system (the Hill coefficients were selected to be 5; all other parameters have default values). The dependency for CovS mRNA is not shown since it is identical to that for CovR mRNA. For each curve, the black squares indicate the points of local maximum of the derivative's absolute value.

where m_6 is the Hill coefficient (by default, we take $m_6 = m_{12} = 5$, where m_{12} is the Hill coefficient for binding to the *has* promoter). For the default parameter values, our computations have shown that cooperative binding results in the sigmoidality of signal–response curves (Fig. 9).

We also performed several thousand of computational experiments with the values of binding constants and Hill coefficients (positive integers) selected at random. More than 99% (but not all) of the simulated sets of seven signal–response curves had at least one sigmoidal curve. We did not observe sigmoidality for CovS-P. We performed similar computations for the model with non-cooperative binding, varying the binding constant values and the multiplicities of binding sites. Here, the cases of sigmoidality of signal–response functions occurred, but were less frequent (73% of all cases). Interestingly, in the non-cooperative case only the curves for Has and Has mRNA concentrations could be sigmoidal (and always either both sigmoidal or both hyperbolic). Thus, we conclude that sigmoidality is practically a rule for systems with cooperative binding, and can also be frequently encountered for systems with non-cooperative binding of the regulatory protein. Notably, all sigmoidal curves in the experiments described above had only one local maximum point for the absolute value of the derivative; the curves for CovS-P and CovR-P were strictly monotonically increasing, while the curves for all other variables were strictly monotonically decreasing.

While the signal detected by the CovR/S system serves as a trigger for the cellular control mechanism, the control itself is effected by the transcription regulator, CovR-P. It is thus of interest to investigate another type of signal–response curve, the one in which the concentration of CovR-P is plotted against the concentration of the controlled protein (Has) as k_1 changes in a certain range. To obtain this type of dependence, we performed simulations similar to the ones described above. Upon observing sigmoidal behavior we focused only on those cases in which sigmoidality was sufficiently pronounced so that the local maximum of the absolute value of the derivative was above a threshold chosen to be $\tan(\pi/6) = 0.577$. As a result, we found that sigmoidality was typical for cooperative systems (94% of the curves were above-threshold sigmoidal), while hyperbolicity was more typical for non-cooperative ones (46% of curves were above-threshold sigmoidal). All curves were monotonically decreasing, and all sigmoidal curves had only one local maximum point for the absolute value of the derivative.

For the cooperative system mentioned above, and also for the system with no cooperativity (varying the multiplicity of the "Has"-like binding sites for CovR-P instead) we have plotted the sigmoidality graphs for different values of the Hill coefficients and the coefficient K_{12}. The plots in Fig. 10 show the dependency of the local maxima of the absolute value of the derivative on these parameters for the cooperative case. In the non-cooperative case, the picture is similar (data not shown).

4.3. Analysis of the reduced model

The complexity of the full model (1)–(8) makes its analytic investigation unfeasible. Therefore we attempted to identify a simpler, analytically tractable version of the initial model by model reduction, setting the rate constants of the reactions, which can be eliminated from the model without changing the model's dynamics, equal to 0. We identified such reactions using sensitivity analysis (Heinrich and Schuster, 1996; Varma et al., 1999) as described in

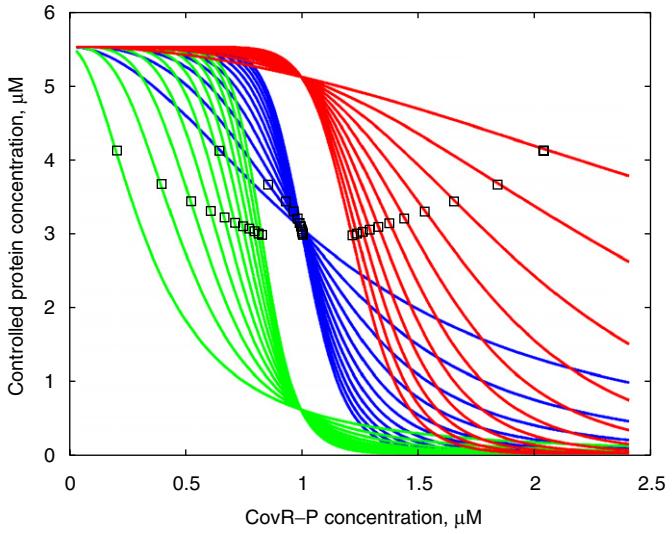

Fig. 10. Cooperative case; different values of m_{12} (Hill coefficient) and K_{12} (binding constant) for *has* promoter binding to CovR-P (all parameters had default values). The parameter m_{12} varies from 2 to 12. Green: $K_{12} = 8$; blue: $K_{12} = 0.8$; red: $K_{12} = 0.08$. For each value of K_{12}, the steepest curve corresponds to the maximum m_{12}. For each curve, the black square denotes the point of local maximum of the derivative's absolute value.

Methods. The remarkable advantage of this reduced model comes from the fact that certain aspects of the reduced model's steady-state behavior can be studied analytically; see Appendix A for details. We were able to obtain an explicit expression for k_1 as a function of the steady-state concentration of X_3 (CovR concentration); that function is monotonically decreasing. The monotonicity implies that the inverse of this function uniquely defines the function $X_3(k_1)$. Since all other concentrations can be uniquely expressed in terms of X_3, we came to the conclusion that the reduced system has a unique positive steady state solution. The main result of the analytic investigation was our proof that the signal–response functions $X_1(k_1)$, $X_3(k_1)$, $X_4(k_1)$, and $X_5(k_1)$ (the concentrations of CovS, CovR, CovR-P, and CovR mRNA, respectively) for the reduced non-cooperative system cannot be sigmoidal for all possible rate and equilibrium constant values, and arbitrary binding site multiplicities.

5. Discussion

We have developed a DDE model of the CovR/S signal transduction/transcription regulation system in *S. pyogenes*, and investigated its properties. We have identified the major features of the dynamic behavior of the system: existence, uniqueness and stability of the steady state, and the possibility of oscillations. While the oscillations arise as a consequence of increased delays in the system, even relatively small delays cause noticeable differences between the dynamics of the DDE and the corresponding ODE systems. In the case of small delays, the long-term dynamics of the DDE system may be well approximated by that of the system without delays.

The existence and uniqueness of the steady state indicates that, in the case of the CovR/S system, evolution has chosen a straightforward way of developing a molecular sensor. Systems with a unique steady state demonstrate the simplest possible limiting behavior (as opposed to sustained oscillations, multistability, hysteresis, chaos, etc.). Apparently, in the case of a two-component system such as the CovR/S system this simplicity is sufficient for functionality. Moreover, memory-like properties such as hysteresis and irreversibility, that can be observed in more complex bistable systems (Ferrell, 2002), may in fact be deleterious in a system designed to promptly detect the current state of the microenvironment. In a CovR/S-type system with a unique steady state, an additional advantage comes from the versatility of the steady-state response, which can be of both hyperbolic (gradual) and sigmoidal (switch-like) types, depending on the parameter values. We also suggest that systems with simpler dynamics are easier to integrate into complex biochemical networks. If this is correct, features like unique steady state should be expected in many elementary biochemical blocks that the sophisticated molecular machinery of the living cell comprises.

The biological role of oscillatory behavior in two-component transduction systems remains to be uncovered. Probably the best-known system where oscillations evidently perform a biological function is the circadian clock (Lema et al., 2000; Sriram and Gopinathan, 2004). There, biochemical oscillations reflect the relationship between the cellular processes and the environmental light–dark cycle with period 24 h. In other biochemical systems, e.g., the glycolytic pathway (Garcia-Olivares et al., 2000), oscillations appear to be present primarily as a benign consequence of the structure and the parameter values of the system. The currently available knowledge about signal transduction systems does not allow us to point out a particular functional advantage that oscillations *per se* may provide. Therefore, they seem to be a collateral result of the action of evolutionary factors that maintain the functionality of the system in the specific biochemical context. Evidence exists that oscillations can arise in the signal transduction systems responsible for chemotaxis as a result of a mutation, thus being an anomaly (Rao et al., 2004). The role of oscillations in the CovR/S system will be clarified when more experimental data on the dynamics of the system under different conditions will be available.

Being a two-component regulatory system with a feedback loop, the CovR/S system can be viewed as consisting of two functional modules. One of these modules centers around CovS and is responsible for signal transmission, and the other module is the gene expression control module containing the negative feedback loop. This module representation has a clear intuitive meaning. Recently, modular analysis of biological systems has attracted much attention, as it can simplify the investigation of large

complex systems once the behavior of the constituent modules is well understood (Saez-Rodriguez et al., 2004; Saez-Rodriguez et al., 2005).

In the case of the CovR/S system, a natural question is to what extent the behavior of the complete system is determined by the properties of the transcription regulation module. This question can be answered by comparing the behavior of the CovR/S system model with that for a one-gene expression control system with a negative feedback. The equations for this system have the form

$$\mathrm{d}M(t)/\mathrm{d}t = a/(1 + KP(t - \tau_1))^5 - bM(t), \tag{21}$$

$$\mathrm{d}P(t)/\mathrm{d}t = cM(t - \tau_2) - dP(t), \tag{22}$$

where M and P are the concentrations of the mRNA and the protein, respectively, and a, b, c, d, K are positive constants.

Our experiments with system (21)–(22) demonstrated (data not shown) that its unique steady state is stable, and that oscillations are possible, tending to be more pronounced as the delay times increase (for zero delays there are no oscillations). Similar results concerning systems akin to Eqs. (21)–(22) were obtained earlier (Griffith, 1968a, b; Banks and Mahaffy, 1978; Bliss et al., 1982; Smith, 1987; Jensen et al., 2003). It is clear from our description of the CovR/S system dynamics that the above features are characteristic of the two-component system model as well. Thus, the major behavioral features such as uniqueness and stability of the steady state and the possibility of oscillations for large delays are shared by both the CovR/S model and the simple transcription regulation system. It seems plausible that these features are generally determined primarily by the transcription regulation modules of two-component systems, and thus can be predicted from the analysis of the simplified one-protein model similar to Eqs. (21)–(22). We conjecture that this pattern holds for all types of prokaryotic two-component systems with negative feedback.

The behavior of signal transduction systems having a single steady state in response to jump-like changes in signal intensity served as a basis for classifying the systems into four categories: systems with no adaptation, with partial adaptation, complete adaptation, and over-adaptation (Koshland et al., 1982; Asthagiri and Lauffenburger, 2000). If an increase in the signal results in an increase in the value of the response variable, then, in systems with no adaptation, the response grows monotonically until it reaches a new steady-state value. In systems with partial adaptation, the value of the response variable grows with an overshoot and then settles at a new steady state. In systems with complete adaptation, the new steady state value for the response variable is the same as the one before the jump, so the increase in the value of the response variable is transient. Systems with over-adaptation can be characterized as the ones whose new steady-state response value (after an overshoot) is lower than the one before the jump. Our modeling results (Fig. 4) show that the CovR/S system is a system with partial adaptation for some of the variables (e.g. [CovR-P], [CovS-P]) and (almost) no adaptation for others (e.g. [CovR]). Koshland et al. (1982) suggested that this is the type of response to be expected in a system which combines a negative feedback loop with delays; our studies confirm this suggestion. While it is unclear what signal is transduced by the CovR/S system, the type of response can shed light on the nature of the signal. Partial adaptation was described as a response type which is suitable for systems that do not need a very high level of sensitivity. Systems that do, e.g., the ones involved in chemotaxis, demonstrate complete adaptation response. This observation indicates that the systems which, like the CovR/S system, include a negative feedback loop and delays, are unlikely to participate in chemotaxis (and, probably, in other type of taxis) reactions. In mammals, partial adaptation is characteristic of hormonal signaling (Koshland et al., 1982). If the CovR/S system triggers the GAS cell's transition to virulence in response to chemical changes in the surrounding environment, we may conjecture that partial adaptation is often a property of prokaryotic and eukaryotic signal transduction systems responsible for the detection of chemical substances which have a potential to induce profound changes in the cell's metabolism. This conjecture may serve as a guideline when analyzing the yet unknown role of signal transduction systems with known dynamical properties.

In certain mammalian signal transduction systems, the transition between different response levels is facilitated by bistability (Ferrell and Xiong, 2001; Ferrell, 2002; Tyson et al., 2003; Angeli et al., 2004). In such systems, the adaptation mechanism is irrelevant (Koshland et al., 1982). To exhibit bistability, a system must possess certain structural properties such as a positive (or double-negative) feedback loop (Ferrell, 2002). The two-component bacterial signal transduction system studied by Kremling et al. (2004) did not exhibit bistability. Probably, monostability is a typical property of bacterial two-component signal transduction, reflecting the general "simplicity" of bacteria compared to eukaryotic organisms. However, it can be shown that adding a second negative feedback loop to the CovR/S-type system is sufficient for bistability. Real-life examples of such systems are yet to be found.

Multistability in a signal transduction system manifests itself in several response levels. Monostable systems can exhibit several response levels due to sigmoidality. As cooperative binding is described by sigmoidal binding curves, it is possible to hypothesize that cooperative binding leads to sigmoidal signal–response curves. Our results show that this association indeed holds, especially for cooperative systems, but only on the average, and with certain exceptions.

Particularly, rigorous treatment of formally defined sigmoidality (with k_1 as the independent variable) in the simplified model of the non-cooperative CovR/S system allowed us to conclude that sigmoidality is impossible for the concentrations of CovS, CovR, CovR-P, and CovR

mRNA as functions of k_1. The simulations show that the same statement holds for the full non-cooperative model. On the other hand, in the non-cooperative case the sigmoidal behavior is rather typical for Has mRNA and Has. This fact explains the difficulties in analytical treatment of these variables, since the type of system behavior depends on the parameter values along with the model structure rather than on the model structure alone.

For [Has] vs. [CovR-P] response curves (Fig. 10), sigmoidality seems to be typical for cooperative systems, and quite frequent for non-cooperative ones. In general, signal–response curves of sigmoidal type are associated with elevated sensitivity and more precise control (Koshland et al., 1982). The close association of cooperativity and sigmoidality suggests that cooperative binding can be favored in evolution if the sigmoidality feature of signal–response curves is to be selected.

Not only did the sensitivity-based simplification procedure allow us to give analytical treatment to the properties of the signal–response characteristics, but it also made it possible to analyze the interactions of the CovR/S system with other biochemical pathways in the cell. This can be illustrated by the analysis of the role of the external phosphoryl donor X-P in the dynamics of the CovR/S system. X-P is assumed to be a small molecule, a standard element of the cell's normal metabolism, such as acetyl phosphate AcP (we used the data from Blat et al., (1998) on AcP phosphorylation of CheY to derive the value for k_3). While the rate of phosphorylation of CovR by X-P is relatively high, the dynamics of the CovR/S system is insensitive to changes in the intensity of this process. This fact sheds light on the role of phosphorylation by the external donor. In normal cells, CovS-P is always present, and we see that in this situation phosphorylation by X-P has negligible influence. Therefore, one reasonable suggestion is that phosphorylation by X-P is a result of some crosstalk between phosphorylation circuits, which was conserved in evolution in the presence of negative or neutral selection. Therefore, the analysis of sensitivities of the system to perturbations may lead to insights into the evolution of biological functional systems.

As already mentioned, our model describes the dynamics of the signal transduction system averaged over a population of cells, or in a cell-free extract containing all necessary biochemical components. To improve our understanding of the dynamics of signal transduction systems in bacteria, it is necessary to model the signal transduction/transcription regulation processes occurring in a single cell. Such a description cannot be obtained using the ODE/DDE formalism, since the numbers of molecules for some of the chemical species involved are so small that their stochastic fluctuations need to be taken into account. Therefore, a stochastic model for the CovR/S system needs to be developed. While the traditional Markov stochastic modeling methodology does not allow the introduction of delays into the stochastic system, a probabilistic approach to modeling chemical systems with delays was recently proposed (Bratsun et al., 2005). A stochastic model will allow us to investigate the role of fluctuations in signal transduction, in order to see to what extent random events can cause the system's self-excitation leading to behavioral response on the cellular level.

In conclusion, we would like to emphasize the generality of our approach. Conventional approaches to modeling signal transduction have recently been criticized for generating knowledge about specific systems which is not easily convertible to knowledge about other types of signal transduction systems (Soyer et al., 2006). Our approach does not suffer from this shortcoming, as it allows us to generate reasonable hypotheses concerning other systems and provides means to test these hypotheses. To investigate the properties of the CovR/S two-component signal transduction in *S. pyogenes*, we have developed a new methodology applicable to a broad range of signal transduction systems. The essential features of our approach are: (a) explicit use of transcriptional and translational delays; (b) development of an efficient procedure to find the steady-state solution to the dynamic equations, which allowed us to construct steady-state signal–response curves; (c) use of a rigorous and general definition of sigmoidality; (d) use of sensitivity analysis to reduce the full model to a model which can be investigated analytically. The natural next step is to apply our methodology to two-component systems with positive feedback and systems of other types.

Acknowledgments

Work at Emory was supported by NIH Grant AI20723 to June R. Scott. AYM and MB were supported in part by NIH Grant HG00783 to MB.

Appendix A. Analysis of the signal–response curves for the reduced model

Here we formulate and prove the mathematical results concerning the CovR/S system model obtained as a result of system reduction. The first four steady-state equations for the reduced system are as follows:

$$k_2X_2X_3 + k_5X_2 + k_{10}X_5 = k_1[\mathrm{ATP}]X_1 + k_{11}X_1, \tag{A.1}$$

$$k_2X_2X_3 + k_5X_2 = k_1[\mathrm{ATP}]X_1, \tag{A.2}$$

$$k_2X_2X_3 + k_9X_3 = k_4X_4 + k_8X_5, \tag{A.3}$$

$$k_2X_2X_3 = k_4X_4. \tag{A.4}$$

The remaining three equations coincide with Eqs. (13)–(15). We first concentrate on system {(A.1)–(A.4), (13)} for X_1, X_2, X_3, X_4, and X_5.

Eqs. (A.1)–(A.4) imply that Eqs. (16) and (17) hold. Combining Eq. (A.2) with Eqs. (16) and (17), we get

$$X_3 = \frac{k_5X_2}{k_1\alpha - k_2X_2}, \tag{A.5}$$

where $\alpha = [ATP]k_{10}k_9/(k_{11}k_8)$. Using Eq. (A.4) together with the expression for X_4 obtained from Eqs. (13) and (17), we obtain the formula for X_2:

$$X_2 = \frac{k_4 X_4}{k_2 X_3} = \frac{f(X_3)}{X_3}, \tag{A.6}$$

where

$$f(X_3) = \frac{k_4\left(\sqrt[5]{(k_6k_8/k_7k_9X_3)} - 1\right)}{k_2K_6}.$$

Note that Eq. (A.6) only makes sense if $k_6k_8/(k_7k_9) > X_3$, which is equivalent to $X_5 < k_6/k_6$ (Eq. (19)). Expression (A.6) combined with Eq. (A.5) implies

$$X_3 = \frac{k_5 f(X_3)}{k_1\alpha X_3 - k_2 f(X_3)},$$

which yields

$$k_1 = \frac{k_5 f(X_3) + k_2 f(X_3) X_3}{\alpha X_3^2}. \tag{A.7}$$

Since $f(X_3)$ does not depend on k_1, Eq. (A.7) provides an explicit formula for k_1 in terms of X_3. This equation forms the necessary basis for our analysis of the solution of system {(A.1)–(A.4), (13)}.

Denoting by $h(X_3)$ the right-hand side of Eq. (A.7), we formulate the following proposition.

Proposition 1. *The function $h(X_3)$ is monotonically decreasing for $X_3 \in (0,\ k_6k_8/(k_7k_9))$. Moreover, $h(0) = \infty$, and $h(k_6k_8/(k_7k_9)) = 0$.*

Proof. Follows directly from the definition of $h(X_3)$.

Corollary 1. *System {(A.1)–(A.4), (13)–(15)} has a unique positive solution.*

Proof. Fix arbitrary positive k_1, and consider Eq. (A.7) as an equation in X_3. It follows from Proposition 1 that this equation has a unique positive solution. As follows from Eqs. (13), (16) and (17), the corresponding positive values of X_1, X_4 and X_5 are uniquely determined by X_3. It follows from Eq. (A.2) that

$$X_2 = \frac{k_1[\mathrm{ATP}]X_1}{k_2X_3 + k_5}.$$

This expression implies that X_2 is positive and uniquely defined, if X_3 is. Therefore, system {(A.1)–(A.4), (13)} has a unique positive solution. As follows from Eqs. (14) and (15), the concentrations X_7 and X_8 are uniquely determined by X_5, and are positive if X_5 is.

The equation $X_3 = h^{-1}(k_1)$ describes a signal–response curve for the system. As was discussed in the Results section, one of the most important questions to be asked about such curves is whether they can be sigmoidal. To answer this question for the equation $X_3 = h^{-1}(k_1)$, we will first consider the dependency $k_1 = k_1(X_4)$. Expressions (A.5) and (A.6) yield

$$X_3 = \frac{k_5k_4X_4/(k_2X_3)}{k_1\alpha - k_4X_4/X_3},$$

which implies

$$k_1 = \frac{k_5k_4k_2^{-1}X_4 + k_4X_4X_3}{\alpha X_3^2}. \tag{A.8}$$

Formulas (13) and (17) give $X_3 = \xi(1 + K_6X_4)^{-5}$, where $\xi = k_6k_8/(k_7k_9)$. Plugging this into Eq. (A.8) gives

$$k_1 = \frac{k_5k_4k_2^{-1}X_4}{\alpha\xi}(1 + K_6X_4)^{10} + \frac{k_4X_4}{\alpha\xi}(1 + K_6X_4)^5. \tag{A.9}$$

This formula implies that $k_1 = k_1(X_4)$ is a monotonically increasing function. Therefore, Eq. (A.9) can be inverted, and the uniquely defined function $X_4 = X_4(k_1)$ exists, and is monotonically increasing.

Theorem 1. *The signal–response curve described by $X_4 = X_4(k_1)$ is hyperbolic.*

Proof. Using the definitions of strict convexity and concavity, and the fact that $X_4(k_1)$ is monotonically increasing, it is easy to show that, if $X_4(k_1)$ is strictly convex (concave) on $(k_1^{(1)}, k_1^{(2)})$, then $k_1(X_4)$ is strictly concave (convex) on $(X_4(k_1^{(1)}),\ X_4(k_1^{(2)}))$. Therefore, $X_4(k_1)$ is sigmoidal only if $k_1(X_4)$ is. Strict convexity (concavity) of $k_1(X_4)$ on $(X_4^{(1)}, X_4^{(2)})$ is equivalent to $k_1''(X_4) > 0$ ($k_1''(X_4) < 0$) on this interval, if $k_1''(X_4)$ exists. Therefore, if $k_1''(X_4)$ is continuous, we should have $k_1''(\hat{X}_4) = 0$ for $\hat{X}_4$ separating the interval on which $k_1(X_4)$ is strictly convex from the interval on which it is strictly concave. As follows from Eq. (A.9), $k_1''(X_4)$ is continuous and positive in its domain of definition, which proves the theorem.

Theorem 2. *The signal–response curve described by $X_3 = X_3(k_1)$ is hyperbolic.*

Proof. We can write $k_1(X_3) = F(G(X_3))$, where the function $X_4 = G(X_3)$ is defined by Eqs. (13) and (17), and the function $k_1 = F(X_4)$ is defined by Eq. (A.9). We have

$$k_1'(X_3) = F'(G(X_3))G'(X_3), \tag{A.10}$$

$$k_1''(X_3) = F''(G(X_3))[G'(X_3)]^2 + F'(G(X_3))G''(X_3). \tag{A.11}$$

For appropriately defined constants $\beta, \gamma > 0$,

$$G(X_3) = \beta X_3^{-1/5} - \gamma,$$

which implies $G'(X_3) < 0$ and $G''(X_3) > 0$. From expression (A.9), it follows that $F'(X_4)$, $F''(X_4) > 0$. These facts, combined with Eq. (A.11), show that $k_1''(X_3) > 0$, that is, $k_1 = k_1(X_3)$ is hyperbolic. Formula (A.10) implies that $k_1(X_3)$ is monotonically decreasing. Thus, by the argument similar to the one used in the proof of Theorem 1, we conclude that the inverse function, $X_3 = X_3(k_1)$, also is hyperbolic.

Corollary 2. *The functions* $X_1 = X_1(k_1)$ *and* $X_5 = X_5(k_1)$ *are hyperbolic*.

Proof. Follows from Theorem 2 and the fact that X_1 and X_5 are proportional to X_3.

Remark. Theorems 1 and 2, and Corollary 1 hold for systems analogous to {(A.1)–(A.4), (13)} with arbitrary number, m_6, of non-interacting binding sites for the repressor self-regulation.

Appendix B. Supplementary Materials

The online version of this article contains additional supplementary data. Please visit doi:10.1016/j.jtbi.2006.11.009.

References

Acerenza, L., Mizraji, E., 1997. Cooperativity: A unified view. Biochim. Biophys. Acta 1339, 155–166.

Alves, R., Savageau, M.A., 2003. Comparative analysis of prototype two-component systems with either bifunctional or monofunctional sensors: differences in molecular structure and physiological function. Mol. Microbiol. 48, 25–51.

Angeli, D., Ferrell, J.E., Sontag, E.D., 2004. Detection of multistability, bifurcations, and hysteresis in a large class of biological positive-feedback systems. Proc. Natl. Acad. Sci. USA 101, 1822–1827.

Asthagiri, A.R., Lauffenburger, D.A., 2000. Bioengineering models of cell signaling. Ann. Rev. Biomed. Eng. 2, 31–53.

Asthagiri, A.R., Lauffenburger, D.A., 2001. A computational study of feedback effects on signal dynamics in a mitogen-activated protein kinase (MAPK) pathway model. Biotech. Progr. 17, 227–239.

Banks, H.T., Mahaffy, J.M., 1978. Stability of cyclic gene models for systems involving repression. J. Theor. Biol. 74, 323–334.

Batchelor, E., Goulian, M., 2003. Robustness and the cycle of phosphorylation and dephosphorylation in a two-component regulatory system. Proc. Natl. Acad. Sci. USA 100, 691–696.

Bernish, B., Rijn, I.v.d., 1999. Characterizatin of a two component system in *Streptococcus pyogenes* which is invloved in regulation of hyaluronic acid production. J. Biol. Chem. 274, 4786–4793.

Bhalla, U.S., Iyengar, R., 1999. Emergent properties of networks of biological signaling pathways. Science 283, 381–387.

Blat, Y., Gillespie, B., Bren, A., et al., 1998. Regulation of phosphatase activity in bacterial chemotaxis. J. Mol. Biol. 284, 1191–1199.

Bliss, R.D., Painter, P.R., Marr, A.G., 1982. Role of feedback inhibition in stabilizing the classical operon. J. Theor. Biol. 97, 177–193.

Bratsun, D., Volfson, D., Tsimring, L.S., et al., 2005. Delay-induced stochastic oscillations in gene regulation. Proc. Natl. Acad. Sci. USA 102, 14593–14598.

Cullen, P.J., Bowman, W.C., Kranz, R.G., 1996. In vitro reconstitution and characterization of the Rhodobacter capsulatus NtrB and NtrC two-component system. J. Biol. Chem. 271, 6530–6536.

Cunningham, M.W., 2000. Pathogenesis of group A streptococcal infection. Clin. Microbiol. Rev. 13, 470–511.

Dalton, T.L., Scott, J.R., 2004. CovS inactivates CovR and is required for growth under conditions of general stress in *Streptococcus pyogenes*. J. Bacteriol. 186, 3928–3937.

de Jong, H., 2002. Modeling and simulation of genetic regulatory systems: a literature review. J. Comp. Biol. 9, 67–103.

Endy, D., Kong, D., Yin, J., 1997. Intracellular kinetics of a growing virus: a genetically structured simulation for bacteriophage T7. Biotechnol. Bioeng. 55, 375–389.

Federle, M.J., Scott, J.R., 2002. Identification of binding sites for the group A streptococcal global regulator CovR. Mol. Microbiol. 43, 1161–1172.

Ferrell, J.E., 1996. Tripping the switch fantastic: how a protein kinase cascade can convert graded inputs into switch-like outputs. Trends Biochem. Sci. 21, 460–466.

Ferrell, J.E., 2002. Self-perpetuating states in signal transduction: positive feedback, double-negative feedback and bistability. Curr. Opin. Cell Biol. 14, 140–148.

Ferrell, J.E., Machleder, E.M., 1998. The biochemical basis of an all-or-none cell fate switch in *Xenopus* oocytes. Science 280, 895–898.

Ferrell, J.E., Xiong, W., 2001. Bistability in cell signaling: how to make continuous processes discontinuous, and reversible processes irreversible. Chaos 11, 227–236.

Gao, J., Gusa, A.A., Scott, J.R., et al., 2005. Binding of the global response regulator protein CovR to the *sag* promoter of *Streptococcus pyogenes* reveals a new mode of CovR-DNA interaction. J. Biol. Chem. 280, 38948–38956.

Garcia-Olivares, A., Villarroel, M., Marijuan, P.C., 2000. Enzymes as molecular automata: a stochastic model of self-oscillatory glycolytic cycles in cellular metabolism. Biosystems 56, 121–129.

Goldbeter, A., Koshland, D.E., 1981. An amplified sensitivity arising from covalent modification in biological systems. Proc. Natl. Acad. Sci. USA 78, 6840–6844.

Goodwin, B.C., 1965. Oscillatory behavior in enzymatic control processes. In: Weber, G. (Ed.), Advanced Enzyne Regulation. Pergamon Press, Oxford, pp. 425–438.

Graham, M.R., Smoot, L.M., Migliaccio, C.A., et al., 2002. Virulence control in group A Streptococcus by a two-component gene regulatory system: global expression profiling and in vivo infection modeling. Proc. Natl. Acad. Sci. USA 99, 13855–13860.

Griffith, J.S., 1968a. Mathematics of cellular control processes. 1. Negative feedback to 1 gene. J. Theor. Biol. 20, 202–208.

Griffith, J.S., 1968b. Mathematics of cellular control processes. 2. Positive feedback to 1 gene. J. Theor. Biol. 20, 209–216.

Groisman, E.A., 2001. The pleiotropic two-component regulatory system PhoP-PhoQ. J. Bacteriol. 183, 1835–1842.

Gusa, A.A., Scott, J.R., 2005. The CovR response regulator of group A streptococcus (GAS) acts directly to repress its own promoter. Mol. Microbiol. 56, 1195–1207.

Harshey, R.M., Kawagishi, I., Maddock, J., et al., 2003. Function, diversity, and evolution of signal transduction in prokaryotes. Dev. Cell 4, 459–465.

Hasty, J., McMillen, D., Isaacs, F., et al., 2001. Computational studies of gene regulatory networks: *In numero* molecular biology. Nat. Rev. Genet. 2, 268–279.

Heath, A., DiRita, V.J., Barg, N.L., et al., 1999. A two-component regulatory system, CsrR-CsrS, represses expression of three *Streptococcus pyogenes* virulence factors, hyaluronic acid capsule, streptolysin S, and pyrogenic exotoxin B. Infect. Immun. 67, 5298–5305.

Heinrich, R., Neel, B.G., Rapoport, T.A., 2002. Mathematical models of protein kinase signal transduction. Mol. Cell 9, 957–970.

Heinrich, R., Schuster, S., 1996. The Regulation of Cellular Systems. Chapman & Hall, New York, London.

Hill, T.L., 1985. Cooperativity Theory in Biochemistry: Steady-state and Equilibrium Systems. Springer, New York.

Huang, C.Y.F., Ferrell, J.E., 1996. Ultrasensitivity in the mitogen-activated protein kinase cascade. Proc. Natl. Acad. Sci. USA 93, 10078–10083.

Ingalls, B.P., Sauro, H.M., 2003. Sensitivity analysis of stoichiometric networks: an extension of metabolic control analysis to non-steady state trajectories. J. Theor. Biol. 222, 23–36.

Jensen, M.H., Sneppen, K., Tiana, G., 2003. Sustained oscillations and time delays in gene expression of protein Hes1. FEBS Lett. 541, 176–177.

Kenney, L.J., 2002. Structure/function relationships in OmpR and other winged-helix transcription factors. Curr. Opin. Microbiol. 5, 135–141.

Kholodenko, B.N., 2000. Negative feedback and ultrasensitivity can bring about oscillations in the mitogen-activated protein kinase cascades. Eur. J. Biochem. 267, 1583–1588.

Kholodenko, B.N., Hoek, J.B., Westerhoff, H.V., et al., 1997. Quantification of information transfer via cellular signal transduction pathways. FEBS Lett. 414, 430–434.

Koretke, K.K., Lupas, A.N., Warren, P.V., et al., 2000. Evolution of two-component signal transduction. Mol. Biol. Evol. 17, 1956–1970.

Koshland, D.E., Goldbeter, A., Stock, J.B., 1982. Amplification and adaptation in regulatory and sensory systems. Science 217, 220–225.

Kremling, A., Heermann, R., Centler, F., et al., 2004. Analysis of two-component signal transduction by mathematical modeling using the KdpD/KdpE system of *Escherichia coli*. Biosystems 78, 23–37.

Lema, M.A., Golombek, D.A., Echave, J., 2000. Delay model of the circadian pacemaker. J. Theor. Biol. 204, 565–573.

Mackey, M.C., Santillan, M., Yildirim, N., 2004. Modeling operon dynamics: the tryptophan and lactose operons as paradigms. C. R. Biol. 327, 211–224.

Miller, A.A., Engleberg, N.C., DiRita, V.J., 2001. Repression of virulence genes by phosphorylation-dependent oligomerization of CsrR at target promoters in *S. pyogenes*. Mol. Microbiol. 40, 976–990.

Parkinson, J.S., 1993. Signal transduction schemes of bacteria. Cell 73, 857–871.

Rao, C.V., Kirby, J.R., Arkin, A.P., 2004. Design and diversity in bacterial chemotaxis: a comparative study in *E. coli* and Bacillus subtilis. PLoS Biol. 2, 239–252.

Rao, C.V., Kirby, J.R., Arkin, A.P., 2005. Phosphatase localization in bacterial chemotaxis: divergent mechanisms, convergent principles. Phys. Biol. 2, 148–158.

Rosenfeld, N., Elowitz, M.B., Alon, U., 2002. Negative autoregulation speeds the response times of transcription networks. J. Mol. Biol. 323, 785–793.

Saez-Rodriguez, J., Kremling, A., Conzelmann, H.etal., 2004. Modular analysis of signal transduction networks. IEEE Control Syst. Mag. 24, 35–52.

Saez-Rodriguez, J., Kremling, A., Gilles, E.D., 2005. Dissecting the puzzle of life: modularization of signal transduction networks. Comput. Chem. Eng. 29, 619–629.

Santillan, M., Mackey, M.C., 2001. Dynamic regulation of the tryptophan operon: a modeling study and comparison with experimental data. Proc. Natl. Acad. Sci. USA 98, 1364–1369.

Schoeberl, B., Eichler-Jonsson, C., Gilles, E.D., et al., 2002. Computational modeling of the dynamics of the MAP kinase cascade activated by surface and internalized EGF receptors. Nat. Biotechnol. 20, 370–375.

Smith, H., 1987. Oscillations and multiple steady states in a cyclic gene model with repression. J. Math. Biol. 25, 169–190.

Smolen, P., Baxter, D.A., Byrne, J.H., 2000. Modeling transcriptional control in gene networks—methods, recent results, and future directions. Bull. Math. Biol. 62, 247–292.

Soyer, O.S., Salathe, M., Bonhoeffer, S., 2006. Signal transduction networks: topology, response and biochemical processes. J. Theor. Biol. 238, 416–425.

Sriram, K., Gopinathan, M.S., 2004. A two variable delay model for the circadian rhythm of *Neurospora crassa*. J. Theor. Biol. 231, 23–38.

Stock, A.M., Robinson, V.L., Goudreau, P.N., 2000. Two-component signal transduction. Annu. Rev. Biochem. 69, 183–215.

Sumby, P., Whitney, A.R., Graviss, E.A., et al., 2006. Genome-wide analysis of Group A Streptococci reveals a mutation that modulates global phenotype and disease specificity. PLoS Pathogens 2, 41–49.

Tyson, J.J., Othmer, H.G., 1978. The dynamics of feedback control circuits in biochemical pathways. In: Rosen, R., Snell, F. (Eds.), Progress Theoretical Biology. Academic Press, New York, pp. 1–62.

Tyson, J.J., Chen, K.C., Novak, B., 2003. Sniffers, buzzers, toggles and blinkers: dynamics of regulatory and signaling pathways in the cell. Curr. Opin. Cell Biol. 15, 221–231.

Varma, A., Morbidelli, M., Wu, H., 1999. Parametric Sensitivity in Chemical Systems. Cambridge University Press, Cambridge.

West, A.H., Stock, A.M., 2001. Histidine kinases and response regulator proteins in two-component signaling systems. Trends Biochem. Sci. 26, 369–376.

Yagil, G., Yagil, E., 1971. On the relation between effector concentration and rate of induced enzyme synthesis. Biophys. J. 11, 11–27.

Yildirim, N., Mackey, M.C., 2003. Feedback regulation in the lactose operon: a mathematical modeling study and comparison with experimental data. Biophys. J. 84, 2841–2851.

Yildirim, N., Santillan, M., Horike, D., et al., 2004. Dynamics and bistability in a reduced model of the lac operon. Chaos 14, 279–292.